Int. J. Nanosci. Nanotechnol., Vol. 15, No. 1, March. 2019, pp. 27-36

Application of Multi Flux Model to Predict Optical Performance of Titanium Dioxide Nanopigments

Negin Piri*

Department of R&D, Alyaf Abrisham Mahan Delijan Company, Delijan, Iran.
Faculty of Textile Engineering, Guilan University, Rasht, Iran.

(*) Corresponding author: neginpiri@yahoo.com
(Received: 28 May 2018 and Accepted: 17 September 2018)

Abstract

The area of nano-pigments is a limitless field with exceptional potential applications in industry, and their application is becoming the focus of many research groups worldwide in recent years due to their outstanding and tunable properties. Titanium dioxide (TiO_2) nanoparticles, on the other hand, are among the most widely used pigment particles, and the interest for utilization of these nanoparticles as spectrally selective pigment is continually growing. Accordingly, this contribution utilizes Mie scattering theory and Multi Flux model to study the effect of particle size and concentration on radiative properties and optical performance of TiO2 pigmented coatings in solar spectrum with special emphasis on UV and NIR regions. Optical behaviors of TiO_2 pigments were subsequently evaluated based on AATCC test method 183-2004 for UV-A and UVB regions and standard test method ASTM G 107-03 and ASTM G173-03 for NIR region. At the final step, some experiments have been carried out to evaluate the performance of proposed method.

Keywords: *Titanium dioxide nano-pigments, Pigmented coatings, Radiative properties, Spectral performance, UV shielding, NIR reflectance.*

1. INRODUCTION

In the present era, living standards of the growing world population can no longer be satisfied through conventional means. In this regards, Nanotechnology is a novel expanding area of research involved in manipulating properties and structures at nano scale, which have led to the detailed examinations of different properties of nanostructures as they deviate from those of the bulk material [1-2]. So many works, also, have been contributed on fundamental physics and chemistry for nanoparticle generation with tailored properties via different synthetic methods [3-4].

One of the newest applications of nanoparticles that have been introduced in recent years, is based on their optical properties [5], and is dealt with the alteration of scattering ability of a coated surface in different regions of electromagnetic spectrum [6-7]. This advantage has been utilized to produce materials with desired optical properties such as UV-protection, opacity and NIR reflectance [8-9].

Titanium dioxide (TiO_2) nanoparticle is one of the widely used pigment particles, accounting for almost 70% of the total production volume of pigments worldwide, and the interest for utilization of this nanoparticle in different applications is continually growing due to their extra ordinary optical activity, high availability, nontoxicity, biocompatibility, and low price [10-11]. Accordingly, TiO_2 pigment particles have received growing attention in various industries including but not limited to, building and automobile industry, textile industry and solar cells [12].

TiO_2 nanoparticles exist in three mineral forms including: anatase, rutile, and brookite [13-14], and are known as a wide

band-gap semiconductor that can be excited to produce electron–hole pairs when irradiated with light. Such photo-induced electron–hole pairs have been utilized to create superhydrophilicity, generate electricity in solar cells, to decomposition of water as well as to oxidize and degrade inorganic, organic and biological compounds in environments [15]. On the other hand, it provides whiteness and opacity to products such as paints, plastics, papers, inks, foods, and toothpastes. It can also be found in pharmaceuticals and cosmetic products such as sun-blockers [16-17]. Moreover, TiO_2 nano and sub-micron sized particles have increasingly been used as NIR reflecting pigments in construction, automotive and textile industry [18-19].

It has been widely accepted that, particle size parameter and complex refractive index are two important parameters that influence scattering power of pigment particles [20-21]. Accordingly, a systematic investigation and a deep knowledge on the relationship between radiative properties of TiO_2 pigment particles and their spectral and optical performance allows for a purposeful design of spectrally selective particulate coatings, which would be appropriate for various applications. Accordingly, this study is devoted to investigate the rediative properties and optical performance of TiO_2 nano-pigments, in solar spectrum with a special emphasis on UV and NIR regions.

2. MODEL DESCRIPTION

2.1. Mie Scattering Calculations

There There are rigorous and approximate methods for performing light scattering computations from small particles, among them, Mie scattering theory is a versatile route for calculation of scattered light from homogeneous spherical particles of arbitrary size, irradiated by the electromagnetic wave, whose wavelength is in the order of the particle size [22]. Mie calculations were performed in order to calculate radiative properties of TiO_2 nano-pigments with 35, 120 and 250 nm, embedded in non-absorbing medium, with n=1.54. In order to do that, literature-based complex index of refraction, within the range of (300-1100) nm, was used [23].

At the earliest step, using complex refractive index and particle radius as input parameters, the cross sections for extinction (C_{ext}), scattering (C_{sca}) and absorption (C_{abs}), which are the effective particle cross-sectional areas that encounter a beam of incident radiation, and asymmetry parameter can be calculated performing Mie calculations, and using following formulas [24-2]:

$$C_{sca} = \frac{2\pi}{k^2}\sum_{n=1}^{\infty}(2n+1)(|a_n|^2 + |b_n|^2) \quad (1)$$

$$C_{ext} = \frac{2\pi}{k^2}\sum_{n=1}^{\infty}(2n+1)Re\{a_n + b_n\} \quad (2)$$

$$C_{abs} = C_{ext} - C_{sca} \quad (3)$$

$$g = \frac{4\pi}{k^2 C_{sca}} Re\sum_{n=1}^{\infty}\left\{\frac{n(n+2)}{n+1}(a_n a_{n+1+}^{*} b_n b_{n+1}^{*}) + 2n+1nn+1anbn*\right. \quad (4)$$

where the expansion coefficients, a_n and b_n, can be expressed in terms of spherical Bessel function as follows:

$$a_n = \frac{\mu m^2 j_n(mx)[x j_n(x)]' - \mu_1 j_n(x)[mx j_n(mx)]'}{\mu m^2 j_n(mx)\left[x h_n^{(1)}(x)\right]' - \mu_1 h_n^{(1)}(x)[mx j_n(mx)]'} \quad (5)$$

$$b_n = \frac{\mu_1 j_n(mx)[x j_n(x)]' - \mu\, j_n(x)[mx j_n(mx)]'}{\mu_1 j_n(mx)\left[x h_n^{(1)}(x)\right]' - \mu_1 h_n^{(1)}(x)[mx j_n(mx)]'} \quad (6)$$

in which, m is the relative refractive index ($m=k/k_1=N/N_1$) and n is the number of iterations which is restricted to only a few terms and is given by the following relation:

$$n_{max} = x + 4x^{1/3} + 2 \quad (7)$$

2.2. Multi Flux Calculations

Multi-flux calculations were performed on pigmented layers with regard to Mudgett and Richard's procedure in treatment of RTE for closely packed

pigmented media [25-26]. Front surface of the media is assumed to be illuminated by ideal diffuse light, which is in the forward direction inside an angle range of ±π/2 and has equal energy over the entire range of these angles. A polar coordinate system of 26 unequal angular segments, which covers different ranges of angles from perpendicular to horizontal, was constructed, according to figure 1, to describe the angular distribution of the radiation intensity which is passing through the medium [27-28].

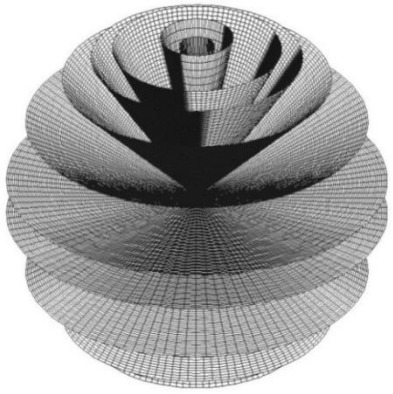

Figure 1. *Space discretization for multi-flux model.*

The energy balance on each segment will result in 26-coupled simultaneous first order differential equations as follow:

$$\frac{\partial F(\tau,\mu)}{\partial z} = \frac{-k_{ext}}{\mu} F(\tau,\mu) + k_{sca} \int_{4\pi} \frac{F(\tau,\mu')}{\mu'} \frac{p(\mu,\mu')}{4\pi} d\omega' \quad (8)$$

The first term in right hand side of above equation represent loss by scattering and absorption in direction μ, and the second term denote the gain by scattering from all other directions, μ', towards direction μ. Equation 8 can be written in the matrix form as:

$$\begin{cases} \frac{dF_i}{d\tau} = \sum_{j=1}^{n} S_{ij} F_j & i \le n/2 \\ -\frac{dF_i}{d\tau} = \sum_{j=1}^{n} S_{ij} F_j & i \ge n/2 \end{cases} \quad (9)$$

in which,

$$S_{ij} = \frac{\varphi_i}{4\pi|\cos\theta_j|} \sum_{l=0}^{L} a_l P_l(\cos\theta_i) P_l(\cos\theta_j) \quad for\ i \neq j$$

$$S_{jj} = -\frac{k_{abs}/k_{sca}}{|\cos\theta_j|} - \sum_{m=1, m\neq j}^{n} S_{mj} \quad for\ i = j \quad (10)$$

where, k_{sca} and k_{abs} are scattering and absorption coefficients respectively and are measured from:

$$k_{abs} = \frac{3\pi Q_{abs}}{2\lambda x} \quad and \quad k_{sca} = \frac{3\pi Q_{sca}}{2\lambda x} \quad (11)$$

in which, Q_{abs} and Q_{sca} are efficiency parameters for absorption and scattering respectively, and a_l are Legendre coefficients.

Equation 9 has the general solution of:

$$F_i = \sum_{j=1}^{n} A_{ij} C_j exp(L_j \tau) \quad i \in [1, n] \quad (12)$$

where F_i is the monochromatic flux contained in channel i, τ is optical thickness, A denotes the eigenvectors of the matrix S, L is the corresponding eigenvalues, and C is the constant determined by fitting the boundary conditions.

Subsequently, the reflection and transmission of the layer was obtained from:

$$R = \sum_{i=1}^{n/2} F_i \ and \quad T = \sum_{i=n/2}^{n} F_i \quad (13)$$

and the absorbance of the samples is simply calculated by following relationship:

$$A_\lambda = 1 - R_\lambda - T_\lambda \quad (14)$$

2.3. UV Shielding of TiO_2 Pigments

The UV-protection efficiency of all samples was examined using Ultraviolet Protection Factor (UPF). A higher UPF value represents the greater protection level. The UPF values of all samples were calculated according to AATCC test

method 183-2004 for UV-A (315–400 nm) and UVB (280–315 nm) from the transmittance data, and using:

$$UPF = \frac{\sum_{\lambda_2}^{\lambda_1} E_\lambda \times S_\lambda \times \Delta\lambda}{\sum_{\lambda_2}^{\lambda_1} E_\lambda \times S_\lambda \times T_\lambda \times \Delta\lambda} \quad (15)$$

where E_λ is relative erythemal spectral effectiveness, S_λ is solar spectral irradiance, T_λ is average spectral transmittance of specimen and $\Delta\lambda$ represents wavelength interval. $\lambda 1$ and $\lambda 2$ in equation 1 denotes (290 nm and 315 nm) for UVB, and (315 nm and 380 nm) for UVA regions, respectively. In addition, the average ultraviolet transmittance of the samples can be calculated as follow:

$$T(UVA\ or\ U) = \frac{\sum_{\lambda_2}^{\lambda_1} T_\lambda \times \Delta\lambda}{\sum_{\lambda_2}^{\lambda_1} \Delta\lambda} \quad (16)$$

Classification of sun protection properties of all samples has been performed based on protection level and transmittance and according to table 1 [29].

2.4. NIR Reflectance of TiO_2 Nano-pigments

By using reflectance spectra of the samples in solar spectrum, it is possible to calculate NIR reflectance percentage, which is a measure of heat rejection in NIR region and is specified as:

$$\rho_{NIR} = \frac{\int_{\lambda_1}^{\lambda_2} \rho_\lambda I(\lambda) d\lambda}{\int_{\lambda_1}^{\lambda_2} I(\lambda) d\lambda} \quad (17)$$

where, $\rho(\lambda)$ is the spectral reflectance of the sample, $I(\lambda)$ is the solar irradiation in λ_1=(7000) nm to λ_2=(1100) nm wavelength region, as is proposed in standard test method ASTM G 107-03 and [30].

3. EXPERIMENTAL PROCEDURE

3.1. Materials

Raw white 100% Taffeta weaved polyester fabric, (310 g/m^2), was selected as substrate, and was kindly supplied with Berelian Mahtab Baft Company, and was used in all the experiments.

Table 1. *Classification of UPF based on protection level and transmittance.*

UPF	T(UVB)	Protection category
Less than 15	More than 6.7	Insufficient protection
15-24	6.7-4.2	Good protection
25-39	4.1-2.6	Very good protection
40-50, 50+	Less than 2.5	Excellent protection

Titanium dioxide with rutile structure and average particle size of 35 nm, 120 nm and 250 nm was purchased from Nobond technologies Co, China. Distilled water has been provided in the laboratory of Guilan University.

3.2. Coating of Polyester Fabric

Various amounts of TiO_2 nanoparticles, namely 0, 1, 2, 3 and 4 wt.% were dispersed in distilled water and the mixture was sonicated for 15 minutes using a Branson Sonifier 250, operated at 30 W, in order to prepare a homogeneous dispersion of TiO_2 nano-pigments.

Polyester fabrics with different colors, namely, white, red, yellow and blue, were immersed in resulting dispersion with a liquid to good ratio of 10:1 at room temperature for 30 min and then the excessive amount of solution was removed from the samples through a padding process. To this end, a horizontal automatic padding machine with the nip pressure of 1.0 kg cm^{-2} and 100% pick up was used. This process was followed by a drying step at 100 °C for 4 min and curing process at 140 °C for 5 min using a Pad-thermosol machine.

3.3. Characterization

The morphology of nano-pigments on polyester fabric was analyzed through the

high resolution FESEM images taken by MIRA3 TESCAN. The impact of coating with TiO_2 nano-pigment on the reflectance of polyester substrate was analyzed utilizing SPECORD 250 - 222P168 spectrophotometer in 200-1100nm wavelength.

The temperature measurement of lower surface of reference and coated polyester fabrics under the NIR irradiated condition was performed using heat box, which has been prepared based on ASTM D 4803–97 standard test method [31]. The 10×10 control and TiO_2 coated fabrics were placed on a sample holder and exposed to NIR radiation using NIR lamp (250w, 230v, 1.1A and color temperature of 6000K), simultaneously. The distant between sample and NIR lamp was set to be 50 cm. Figure 2 shows a schematic of the thermometric experiment. The temperature inside the box was set to 18 °C using an air conditioner.

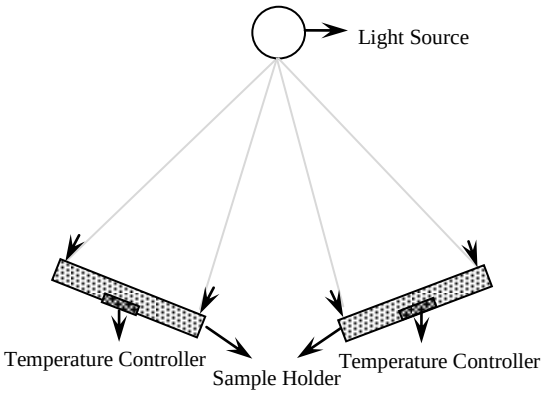

Figure 2. *Schematic of experimental apparatus for heat box.*

Obtained results from the heat box were reported in the form of produced temperature difference (ΔT) between temperature of control ($T_{control}$) and coated sample (T_{sample}) measured as:

$$\Delta T = T_{control} - T_{sample} \qquad (18)$$

4. RESULTS AND DISCUSION

4.1. Radiative Properties of TiO_2 Nanopigments

At the earliest step, Mie calculation was performed in order to calculate the radiative properties of TiO_2 nano-pigments with 35, 120 and 250 nm diameter and in UV, VIS and NIR regions of electromagnetic spectrum. Scattering (Q_{sca}) and absorption (Q_{abs}) efficiencies, which are important parameters that influence the radiative properties of pigments are presented in Figure 3.

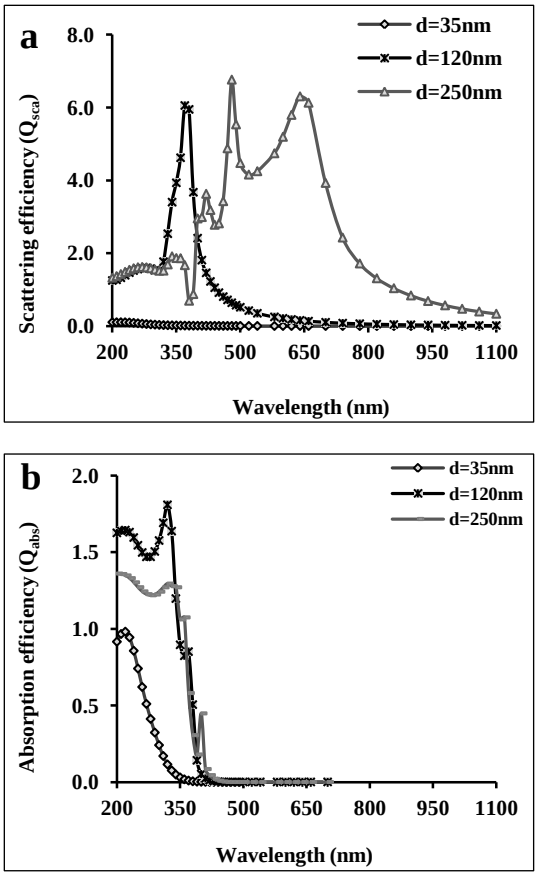

Figure 3. *(a) Scattering and (b) Absorption efficiency of TiO_2 nano-pigments of different particle size.*

As is shown in this figure, with increasing the diameter of nano-pigment from 35 to 120 nm, scattering efficiency of the pigments increases dramatically, but with further increase in particle size to 250 nm, no significant change can be observed in value of maximum scattering efficiency of pigment particles. However, increasing the particle size is resulted in wavelength of maximum scattering efficiency to move towards the larger wavelengths.

Mentioned remarks reflect the fact that, TiO_2 nano-pigments with small diameters

(d=35 nm) have low ability of scattering the incident radiation, whereas, by increasing particle size to 120 nm and larger, ability of particles in scattering of incident radiation increases and simultaneously, shifts to NIR region.

In addition, absorption efficiency, Q_{abs}, of TiO_2 pigment particles are illustrated in figure 3b. Regarding the figure, Q_{abs} of TiO_2 nano-pigments have their highest value in UV region and decreases dramatically to its minimum value, near zero, at the unset of VIS region. On the other words, Q_{abs} of TiO_2 nano-pigments, except for UV wavelengths, is negligible over solar spectra, which shows that, TiO_2 nano-pigment is non-absorbing in VIS and NIR regions.

4.2. Spectral Behavior of TiO_2 Nano-pigments

Reflectance and transmittance mono-dispersed TiO_2 nano-pigments, embedded in non-absorbing resin with n=1.54 and thickness of 1500 µm has been calculated using MF model and the results is presented in Figures 4. It is clear from these figures that, Titanium dioxide nano-pigments are highly absorbing in UV region and nearly nonabsorbing in VIS and NIR regions. With regards to Figure 4a reflectance of nano-pigments has its minimum value in UV region. A sudden increment can be observed in reflectance spectra of TiO_2 nano-pigments at the onset of VIS region, which is attributed to the sharp decrease in imaginary part of refractive index. An increase in reflectance arises with increasing the particle size from 35nm to 250 nm. Regarding Figure 4b, roughly same behavior can be observed in transmittance of TiO_2 nano-pigments. In transmittance spectra, a spectral band at around 200-450 nm with nearly zero transmittance value can be clearly recognized. With increasing wavelengths, transmittance of TiO_2 nano-pigments experiences an increase to its maximum value and then reaches a plateau.

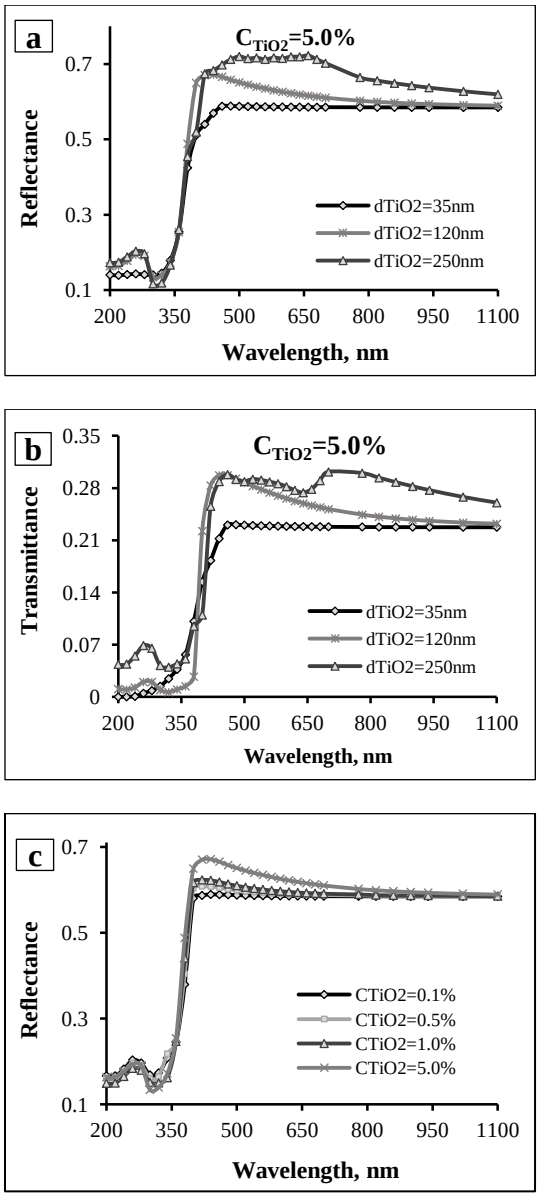

Figure 4. *(a,c) Reflectance and (b) Transmittance of TiO_2 nano-pigments with different diameters.*

4.3. UV Shielding of TiO_2 Nano-pigments

Figure 5 presents the measured UPF and T(UVA, UVB) of TiO_2 pigments with d_{TiO2}=35, 120 and 250 nm. Figures 5a-c show that, at the same condition, by increasing the volume fraction, UPF of the pigmented layer increases and at the same time T(UVA/UVB) decreases.

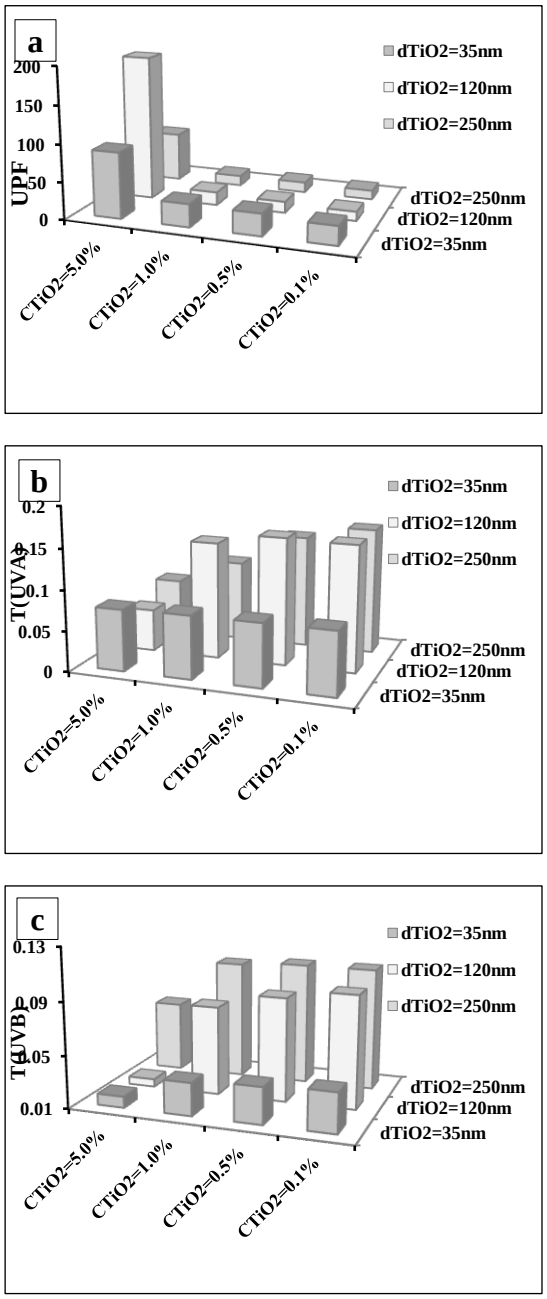

Figure 5. *(a) UPF, (b) T(UVA) and (c) T(UVB) of TiO_2 nano-pigments with various diameters.*

Furthermore, at small volume fractions, (0.1-1.0)%, UPF of the pigmented coating increases as particle size, d_{TiO2} , increases. At higher volume fractions, UPF has the maximum and minimum values in the case of particles with d_{TiO2}=120 nm and d_{TiO2}=250 nm, respectively. Regarding to Figures 5b and c, roughly reverse trend can be observed in transmittance of pigmented layer in UVA and UVB regions. Presented results in Figures 5(a-c) imply that, TiO_2 nano/micro pigments with diameter in the range of (35-250) nm, has very small transmittance in UVA and UVB regions, and large UPF especially in the case of greater volume fractions and smaller diameters. This feature put TiO_2 pigment particles with d_{TiO2}=35 nm in very good to excellent protection category.

4.4. NIR Reflectance of TiO_2 Nano-pigments

NIR reflectance of TiO_2 nano-pigments are illustrated in Figure 6. With regards to Figure 6, a considerable increase can be observed in NIR reflectance of TiO_2 pigment particles by increasing the volume fraction and particle size. These results imply the power of TiO_2 pigment particles in mitigation of thermal heating as a result of absorption of NIR irradiation.

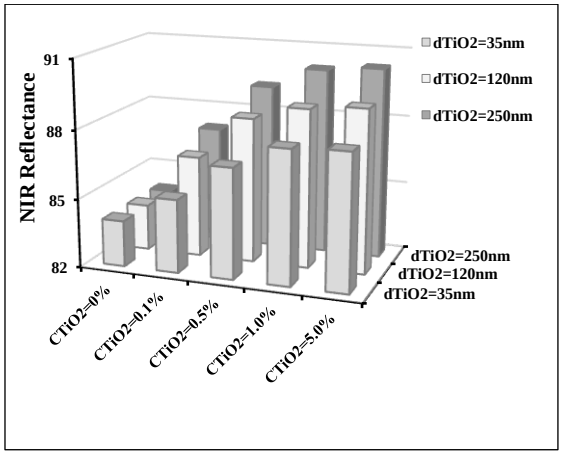

Figure 6. *NIR reflectance of TiO_2 nano-pigments.*

According to observed results TiO_2 pigments with d_{TiO2}=250 nm are the best choice as cool pigments and those with d_{TiO2}=35 nm are worst choice for this purpose.

5. Experimental Evaluation of the Model

Coated polyester fabrics with TiO_2 nano and sub-micron sized pigments with 35, 120 and 250 nm in diameter and different concentrations were selected to evaluate NIR reflectance and cooling performance of TiO_2 pigments.

Figure 7 represents a clear perspective of successful incorporation of TiO_2 particles to the surface of polyester fabrics. Some agglomerations can, also, be observed. Temperature difference between control and coated fabrics- with different shades, namely white, red, blue and yellow- has been measured at steady state (30 minutes after exposure to NIR radiation) according to equation 18, and the results are summarized in table 2.

According to obtained results, an average temperature difference in the range of (0.95-4.90)°C can be obtained as a result of coating of polyester fabrics with TiO_2 nano-pigments.

In addition, at the same particle diameter, ΔT increases by increasing the pigment concentration from 1 to 3 g/lit. Further increase in concentration of TiO_2 pigments does not alter temperature difference noticeably.

Obtained results, also, reveal that, the average temperature difference increases by increasing the particle size from 35 nm to 250 nm. Therefore, submicron sized TiO_2 particles with d=250 nm represents better cooling performance in comparison with pigments with smaller diameter (here, 35 and 120 nm). According to table 2, roughly same trend is observable in coated samples with different shades of color.

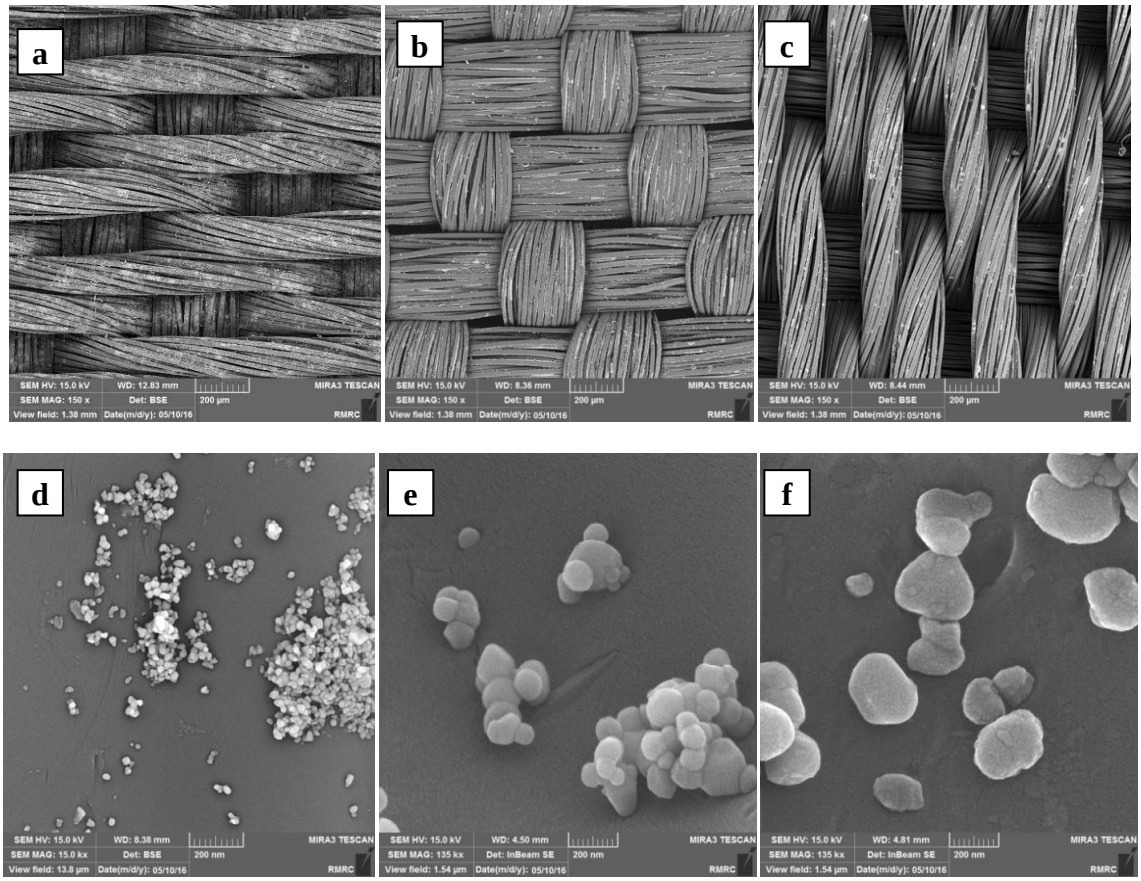

Figure 7. *FESEM micrographs of TiO_2 nano-pigments with (a,d)35nm, (b,e)120nm and (c,f) 250nm in diameter on cellulosic substrate (4.0g/lit).*

Shade of color, on the other hand, has a marginal effect on produced ΔT. Regarding table 2, ΔT is slightly higher in the case of blue samples and slightly lower in the case of white samples.

Presented results in table 2 are in very good agreement with obtained results from Mie-MF model and confirm them at least in NIR region.

6. CONCLUSIONS

Spectral reflectance and transmittance of the spectrally selective TiO_2 nano and submicron sized pigmented coatings with different diameters and concentrations were measured by the means of Mie scattering theory and Multi Flux model. At the further step, UV shielding effect and NIR reflectivity of the pigmented coating were calculated based on AATCC test method 183-2004 for UV-A and UVB regions and standard test method ASTM G 107-03 and ASTM G173-03 for NIR region.

Obtained results from Mie theory revealed that, scattering power of TiO_2 nano and submicron sized pigments increases by increasing particle size and simultaneously shifts towards the larger wavelengths.

In addition, reflectivity of TiO_2 nano-pigments with 35 nm in diameter is smallest in UV region, which yield to very high UPF, and puts the pigments in very good to excellent protection category. UPF of pigmented coating decreases by increasing the particle size to 250 nm.

In contrast, TiO_2 nano-pigments reflect the major part of incident radiation in NIR regions, with the highest value corresponds to larger particle size. Therefore, a TiO_2 pigment with 250 nm in diameter is the best choice as a cool pigment. Obtained results are in very good agreement with experimental observations.

Table 2. *produced temperature between control and coated samples irradiated by NIR radiation*

Particle diameter	Pigment concentration	Average ΔT			
		White Samples	Red Samples	Blue Samples	Yellow Samples
35 nm	0	0	0	0	0
	1	0.95	1.00	1.20	1.00
	2	1.40	1.45	1.60	1.40
	3	1.70	1.75	1.90	1.70
	4	1.90	2.00	2.30	1.95
120 nm	0	0	0	0	0
	1	1.45	1.50	1.65	1.50
	2	2.00	2.10	2.20	2.00
	3	2.35	2.40	2.55	2.40
	4	2.60	2.70	2.90	2.80
250 nm	0	0	0	0	0
	1	2.70	2.65	2.70	2.60
	2	3.35	3.40	3.65	3.40
	3	4.10	4.10	4.35	4.20
	4	4.50	4.50	4.90	4.65

REFERENCES

1. Piri, N., Shams-Nateri, A., Mokhtari, J, (2017). "Solar spectral performance of nanopigments", *Sol. Eng. Mat. Sol. Cell.*, 162: 72–82.
2. Piri, N., Shams-Nateri, A., Mokhtari, J, (2016). " he relationship between refractive index and optical properties of absorbing nanoparticle" *Col. Res. App.*, 41: 477-483.
3. Piri, N., Mottaghitalab, V., Arbab, Sh, (2013)." Development and Characterization of MWNTs/Chitosan Biocomposite Fiber," *Fibers. Polym*., 14: 236-242.
4. Farazas, A., Mavropoulos, A., Christofilos, D., Tsiaousis, I., Tsipas, D, "Ultrasound Assisted Green Synthesis and Characterization of Graphene Oxide," *Int. J. Nanosci. Nanotechnol*., 14: 11-17.
5. Akherat Doost, H., Majles Ara, M. H., Koshki, E, "Theoretical Analysis of the Optical Properties of Gold Nanoparticles Using DDA Approximation," *Int. J. Nanosci. Nanotechnol*., 14: 153-158.
6. Gonome, H., Baneshi, M., Okajima, J., Komiya, A., Yamada, N., Maruyama, Sh, (2014). "Control of thermal barrier performance by optimized nanoparticle size and experimental evaluation using a solar simulator*", J. Quant. Spectrosc. Radiat. Transfer*., 149: 81-89.
7. Baneshi, M., Maruyama, Sh, (2016)." The impacts of applying typical and aesthetically–thermally optimized TiO2 pigmented coatings on cooling and heating load demands of a typical residential building in various climates of Iran", *Energ Buildings.*, 113: 99–111.

8. Emam, H. E., Bechtold, T, (2015). ”Cotton Fabrics with UV Blocking Properties through Metal Salts Deposition,” *Appl. Surf. Sci.,* 357: 1878–1889.
9. Guan, Y., Tawiah, B., Zhang, L., Du, C., Fu, Sh, (2014). “Preparation of UV-cured pigment/latex dispersion for textile inkjet printing,” *J Colloid Interface Sci*. *A.,* 462: 90–98.
10. Mirjalili, M., Karimi , L, (2011). “Photocatalytic Degradation of Synthesized Colorant Stains on Cotton Fabric Coated with Nano TiO2,” *JFBI*., 3: 208-215.
11. Radetic, M, (2013). ”Functionalization of textile materials with TiO_2 nanoparticles,” *J. Photochem. Photobiol. Rev*., 16:62– 76.
12. Jafarbeglou, M., Abdouss, M., Ramezanianpour, A. A, (2015). “Nanoscience and Nano Engineering in Concrete Advances”, *Int. J. Nanosci. Nanotechnol*., 11: 263-273.
13. Norouzi, M., Maleknia, L, (2010). “Photocatalytic Effects of Nanoparticles of TiO2 in Order to Design Self-Cleaning Textiles,” *Asian J. Chem.,* 22: 5930-5936.
14. Senić, Ž., Bauk, S., Vitorović-Todorović, M., Pajić, N., Samolov, A., Rajić, D, (2011). “Application of TiO_2 Nanoparticles for Obtaining Self Decontaminating Smart Textiles”, *Sci. Tech. Rev*., 61:63-72.
15. Narayan, H., Alemu, H, (2017). “A Comparison of Photocatalytic Activity of TiO2 Nanocomposites Doped with Zn2+/Fe3+ and Y3+ Ions*”, Int. J. Nanosci. Nanotechnol*., 13: 315-325.
16. Emam, H. E., Bechtold, T, (2015). “Cotton Fabrics with UV Blocking Properties through Metal Salts Deposition”, *App. Surf. Sci*., 357:1878–1889.
17. Guan, Y., Tawiah, B., Zhang, L., Du, C., Fu, Sh, (2014). “Preparation of UV-cured pigment/latex dispersion for textile inkjet printing”, *Colloids Surf A Physicochem Eng Asp,* 462:90–98.
18. Panwar, K., Jassal M., Agrawal, A. K, (2017). “ TiO_2–SiO_2 Janus particles treated cotton fabric for thermal regulation,” *Surf. Coat. Technol*., 309:897–903.
19. Soumya, S., Kumar, N. S., Mohamed, A. P., Ananthakumar, S, (2016). “Silanated nano ZnO hybrid embedded PMMA polymer coatings on cotton fabrics for near-IR reflective, antifungal cool-textiles,” *NJC.,* 40:7210-7221.
20. Shams-nateri, A, “Scattering behavior of nonabsorbing metallic nanoparticles”, *Opt. Laser. Technol*.,44:1670–1674.
21. Piri, N., Shams-nateri, A., Mokhtari, J, (2018). “A novel approach in simulation of spectral reflectance of nanopigment coated fabrics”, *J. Color. Sci. Tech*., JCST-13-07-2017-1746.
22. Wriedt, T, (1998). “a review of elastic light scattering theories”, *Part. Part. Syst. Charact*., 15: 67-74.
23. Palik, E. D, (1991). “Handbook of optical constants of solids”, San Diego: Academic Press.
24. Bohren, C. F., Huffman, D. R, (1983). “Absorption and Scattering of Light by Small Particles”, Wiley-Interscience.
25. Mudgett, P. S., Richards, L. W, (1971). “Multiple Scattering Calculations for Technology”, *Appl. Opt.,* 10:1485-1502.
26. Mudgett, P. S., Richards, L. W, (1972). “Multiple Scattering Calculations for Technology II”, *J. Colloid Interface Sci*., 39: 551-567.
27. Joshi, J. J., Vaidya, D. B., Shah, H. S, (2001). “Application of Multi-Flux Theory Based on Mie Scattering to the Problem of Modeling the Optical Characteristics of Colored Pigmented Paint Films”, *Col. Res. App*., 26: 234-245.
28. El-Zaiat, S. Y, (2013). “Determination of the complex refractive index of a thick slab material from its spectral reflectance and transmittance at normal incidence”, *Optik,* 124:157– 161.
29. AS/NZS 4399. Sun protective clothing e evaluation and classification; 1996.
30. ASTM, ASTM G173-03: Standard tables for reference solar spectral irradiances: direct normal and hemispherical on 37◦ tilted surface, American Society for Testing and Materials, West Conshohocken, PA, 2003.
31. ASTM D 4803-97 (Reapproved 2002), Standard Test Method for Predicting Heat Buildup in PVC Building Products.